involve early transition states resembling π complexes. However, this must also be predicted for the stronger electrophile in the *p*-nitro benzylation reaction. Yet the reaction fits Brown's relationship and this implies a transition state resembling a Wheland (σ complex) intermediate. Thus it appears that the data are more satisfactorily explained with Jencks' approach.

Olah has suggested that in the case of *p*-nitro benzylation meta substitution may have been enhanced through para–meta migration of the σ complex prior to deprotonation. While isomerization is a common Friedel–Crafts side reaction, the following is offered as evidence of its relative unimportance in this reaction: first, if isomerization were occurring, *some* change in product isomer distribution would be expected.[40] None was seen (Table XIII) in *any* run. Second, since the stability of the benzyl cation is a prime factor in intramolecular or intermolecular (disproportionation) migration, the *p*-nitro benzyl group would seem to be the *least* likely to undergo either side reaction. If the *p*-nitro product meta percentage was raised to 22% by isomerization, there should have been some evidence of high meta percentages and/or disproportionation in the other cases.

(40) Olah's idea (Olah, G. A.; Olah, J. A.; Ohyama, T. *J. Am. Chem. Soc.* in press) of deuterium labeling as a test of isomerization is an excellent one. However, even this may not be definitive due to acid-catalyzed hydrogen–deuterium exchange in these systems.

Acknowledgment. This work was supported by the Research Corporation and the National Science Foundation (Grants CHE-7707604, CHE-7915122, PRM-7911225, and NSF-URP). We also thank Professor Leon Stock for a helpful discussion, Harold Thompson for the stirrer design and construction, and Dr. George Cleland for his help in the synthesis of product isomers.

Registry No. $TiCl_4$, 7550-45-0; $SbCl_5$, 7647-18-9; $AlCl_3$, 7446-70-0; C_6H_6, 71-43-2; $C_6H_5CH_3$, 108-88-3; $C_6H_5CH_2Cl$, 100-44-7; *p*-$ClC_6H_4CH_2Cl$, 104-83-6; 3,4-$Cl_2C_6H_3CH_2Cl$, 102-47-6; *p*-$NO_2C_6H_4CH_2Cl$, 100-14-1; *p*-$CH_3C_6H_4CH_2Cl$, 104-82-5.

Study of ^1H Chemical Shifts and Couplings with ^{19}F in 9α-Fluorocortisol. Application of a Novel ^1H–^{13}C Chemical Shift Correlation Technique with Homonuclear Decoupling

Tuck C. Wong,* Venceslav Rutar,† and Jin-Shan Wang‡

Contribution from the Department of Chemistry, University of Missouri, Columbia, Missouri 65211. *Received February 6, 1984*

Abstract: ^1H–^{13}C chemical shift correlation, selective flip of distant protons, and distortionless enhancement by polarization transfer are combined into a new pulse sequence which eliminates most homonuclear *J* couplings. Correlation maps facilitate easy assignments and accurate measurements of ^1H chemical shifts, geminal couplines ($^2J_{HH}$), and heteronuclear couplings with additional spins. The results are obtained without having to resolve the complicated homonuclear multiplets. The study of 9α-fluorocortisol demonstrates the advantages of this method over the conventional chemical shift correlation method. The values of proton chemical shifts, geminal couplings ($^2J_{HH}$), and heteronuclear couplings with fluorine are explained by substitution effects as well as the conformational change of the A ring.

One-dimensional (1-D) ^1H spectra of steroids are very complicated, since resonances of over 20 protons are distributed mostly in a narrow spectral region between 0.5 and 2.5 ppm downfield from Me_4Si. Assignment was possible only for methyl, olefinic, and some other protons shifted signficiantly downfield due to substitution.[1] Therefore, the spectra did not provide much information about the molecular conformation in solution. Recently, Hall and Sanders[2,3] and Barrett et al.[4] used a combination of ^1H two-dimensional (2-D) *J* resolved spectroscopy, NOE differences, and selective homonuclear decoupling to assign the proton spectra of several steroids.

Further information can be obtained from heteronuclear chemical shift correlation NMR[5-8] which separates ^1H and ^{13}C resonances along the F_1 and F_2 dimensions, thus avoiding overlap of peaks and establishing an indispensable link between the spin systems. Although one-bond coupling $^1J_{CH}$ unambiguously correlates chemical shifts and simplifies assignments, the experiments require acquisition of weak ^{13}C signals and measuring times may become unacceptably long. Efficiency of heteronuclear 2-D spectroscopy can be improved by selective proton flips or other spin manipulations[9-13] which suppress "unimportant" interactions.

Table I. Relative Phases of Radio-Frequency Pulses in A and C

step	ϕ_1	ϕ_2	ϕ_3
1	$-y$	x	x
2	$-x$	$-y$	$-x$
3	y	$-x$	x
4	x	y	$-x$

In a previous paper[14] we utilized a combination of ^1H–^{13}C chemical shift correlation and indirect homonuclear decoupling to determine

†On leave of absence from J. Stefan Institute, Ljubljana, Yugoslavia.
‡On leave of absence from Beijing Normal University, Beijing, People's Republic of China.

(1) Bhacca, N. S.; Williams, D. H. "Application of NMR Spectroscopy in Organic Chemistry, Illustration from the Steorid Field"; Prentice Hall: San Francisco, 1964.
(2) Hall, L. D.; Sanders, J. K. M. *J. Am. Chem. Soc.* **1980**, *102*, 5703–5711.
(3) Hall, L. D.; Sanders, J. K. M. *J. Org. Chem.* **1981**, *46*, 1132–1138.
(4) Barrett, M. W.; Farrant, R. D.; Kirk, D. N.; Mersh, J. D.; Sanders, J. K. M.; Duax, W. L. *J. Chem. Soc., Perkin Trans. 2*, **1982**, 105–110.
(5) Maudsley, A. A.; Ernst, R. R. *Chem. Phys. Lett.* **1977**, *50*, 368–372.
(6) Bodenhausen, G.; Freeman, R. *J. Am. Chem. Soc.* **1978**, *100*, 320–321.
(7) Hall, L. D.; Morris, G. A.; Sukumar, S. *J. Am. Chem. Soc.* **1980**, *102*, 1745–1747.
(8) Bax, A.; Morris, G. A. *J. Magn. Reson.* **1981**, *42*, 501–505.
(9) Garbow, J. R.; Weitekamp, D. P.; Pines, A. *Chem. Phys. Lett.* **1982**, *93*, 504–509.
(10) Bax, A. *J. Magn. Reson.* **1983**, *52*, 330–334.
(11) Rutar, V. *J. Am. Chem. Soc.* **1983**, *105*, 4095–4096.

0002-7863/84/1506-7046$01.50/0 © 1984 American Chemical Society

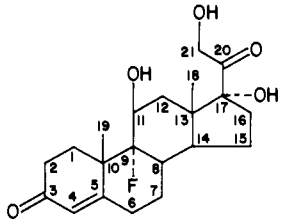

Figure 1. 9α-Fluorocortisol.

proton chemical shifts and geminal couplings progesterone.

Fluorinated steroids are important drugs, and conformational studies in solution are essential for understanding the correlation of their structure and biological activity. It has been pointed out that in 9α-fluorocortisol (**1** in Figure 1) the presence of fluorine substantially changes the conformation of the A ring and enhances the antiinflammatory effect of the drug.[15] 1-D ^1H spectra of fluorinated steroids are mostly unresolvable,[1] and ^{19}F induced chemical shifts of neighboring protons as well as ^1H–^{19}F coupling constants have not been elucidated. The only exception is coupling between ^{19}F and methyl protons.[1]

In this study of **1** we utilize ^1H–^{13}C correlation[12,13] and, in addition to the standard measurement or ^1H chemical shifts, couplings with the ^{19}F spin are determined even without resolving the complicated homonuclear pattern.

Method

Pulse sequence:

$$\begin{array}{l} {}^1H: \ \pi/2(\phi_1)-t_1/2-\pi/2(\phi_2)-\tau-\pi(\phi_1)-\tau-\pi/2(\phi_2)-t_1/2- \\ \qquad\qquad\qquad\qquad \text{evolution} \\ \qquad\qquad\qquad\qquad\qquad\qquad \tau-\pi(\phi_1)-\tau-\theta(\phi_3)-\tau-\text{dec} \\ \qquad\qquad\qquad\qquad\qquad\qquad\quad \text{mixing} \\ {}^{13}C: \qquad\qquad\qquad\qquad\qquad\qquad -\pi(\phi_3)- \\ \qquad\qquad\qquad\qquad \text{evolution} \\ \qquad\qquad\qquad\qquad\qquad\qquad\quad -\pi(\phi_2)- \ -\text{acq}(\pm) \\ \qquad\qquad\qquad\qquad\qquad\qquad\quad \text{mixing} \end{array} \qquad \text{(A)}$$

combines chemical shift correlation with additional pulses

$$\begin{array}{ll} {}^1H: & \ldots\pi/2(\phi_2)-\tau-\pi(\phi_1)-\tau-\pi/2(\phi_2)\ldots \\ {}^{13}C: & \qquad\qquad -\pi(\phi_3)- \end{array} \qquad \text{(B)}$$

at the middle of the evolution time t_1. A four-step phase cycle (Table I) ensures quadrature detection along the F_1 dimension[8] and suppression of coherence transfer echoes.[16]

Since ^{13}C signals of isotopically labeled molecules are detected, protons become divided into two groups. Pulses B apparently do not affect those protons which experience one-bond coupling $^1J_{CH}$ with attached ^{13}C spins, because during the time $2\tau = 1/{}^1J_{CH}$ evolution for 180° compensates effects of radio-frequency pulses.[10-13] On the other hand, distant protons are selectively flipped over; therefore, precession resulting from homonuclear coupling is refocused during the second half of the evolution time.

The subsequent mixing period resembles DEPT[17] with the variable pulse θ which adjusts enhancements of signals of CH_k groups (k = 1, 2, 3). Polarization is transferred into the ^{13}C spin system, and Fourier transformation with respect to the acquisition time t_2 separates carbon chemical shifts (F_2 dimension), while cross sections along the F_1 dimension reveal "manipulated" information about the ^1H spin system which has been evolving during the time t_1.

Pulse sequence A should be compared with the previous approach to homonuclear decoupling in ^1H–^{13}C correlation spectroscopy[12,13]

$$\begin{array}{l} {}^1H: \ \pi/2(\phi_1)-t_1/2-\pi/2(\phi_2)-\tau-\pi(\phi_1)-\tau-\pi/2(\phi_2)-t_1/2- \\ \qquad\qquad\qquad\qquad \text{evolution} \\ \qquad\qquad\qquad\qquad\qquad\qquad \tau-\pi/2(\phi_3)-\tau'-\text{dec} \\ \qquad\qquad\qquad\qquad\qquad\qquad\quad \text{mixing} \\ {}^{13}C: \qquad\qquad\qquad\qquad\qquad\qquad -\pi(\phi_3)- \\ \qquad\qquad\qquad\qquad \text{evolution} \\ \qquad\qquad\qquad\qquad\qquad\qquad\quad -\pi/2(\phi_2)- \ -\text{acq}(\pm) \\ \qquad\qquad\qquad\qquad\qquad\qquad\quad \text{mixing} \end{array} \qquad \text{(C)}$$

where the INEPT version[18,19] of polarization transfer has been used. ^{13}C spins are turned into the xy plane of the rotating frame by the last $\pi/2(\phi_2)$ pulse, and the interval $\tau' \sim 1/(4{}^1J_{CH})$ serves to bring opposite components into phase before they are collapsed onto the F_2 axis by proton decoupling. Obviously, precession resulting from ^{13}C chemical shift dispersion is not refocused, and a phase roll occurs along the F_2 dimension. Precession of the attached protons is also continued during the mixing period, and components with ^1H chemical shift dispersion require different phase corrections after the signals are Fourier transformed with respect to t_1. If single or chemically equivalent protons are attached to the ^{13}C spins, selective flip B suppresses all homonuclear J couplings, and the resulting sharp peaks can be properly phased. In CH_2 groups, however, the protons are often nonequivalent, and geminal coupling ($^2J_{HH}$) is not elminated[13] thus giving rise to four peaks along the F_1 dimension. The phase roll requires extensive corrections of the cross section or magnitude display which may hamper accuracy of results.

Pulse sequence A uses two refocusing π pulses during the mixing period and completely eliminates the phase roll along both dimensions. All cross sections can be displayed in the phase-sensitive mode with minimum correction required. This advantage is offset by the fact that A uses two more pulses than C, and experimental problems associated with inhomogeneous radio-frequency pulses become more severe.

The second advantage of the DEPT mixing period is the inherent possibility of spectral editing which can be accomplished by creating two data sets with $\theta_1 = \pi/4$ and $\theta_2 = 3\pi/4$, respectively. This way, signals of CH_2 and CH groups can be distinguished without significant increase of the measuring time.[17] This advantage is retained even in the case when the refocusing pulses are skipped to reduce spurious peaks arising from inhomogeneous radio-frequency pulses.

The essential improvement of ^1H–^{13}C chemical shift correlation spectroscopy lies in the application of pulses B which are designed to flip only distant protons. There are several apparent obstacles, such as nonuniform values of $^1J_{CH}$, strong coupling in the proton system, etc., which reduce efficiency of the spin manipulation in A or C. However, spurious peaks generally show quite complicated patterns,[13,14] and in most cases their intensity drops below the noise level.

Information which can be derived from the decoupled chemical shift correlation maps is similar to the results of 2-D homonuclear J spectroscopy which also gives rise to proton-decoupled ^1H spectra,[20] but indirect determination of proton chemical shifts via pulse sequences A or C establishes correlation with ^{13}C resonances, and assignments become very reliable. Further advantages are as follows: overlap of peaks is avoided, strong signals of water and other protons which are not bonded to ^{13}C spins do not show up, and strong coupling does not restrict the use of the indirect method.[14] Very high magnetic field is not essential for successful application, and "medium" fields (proton frequencies 200–300

(12) Bax, A. *J. Magn. Reson.* **1983**, *53*, 517–520.
(13) Rutar, V. *J. Magn. Reson.* **1984**, *56*, 87–100.
(14) Wong, T. C.; Rutar, V. *J. Am. Chem. Soc.*, in press.
(15) Weeks, C. M.; Daux, W. L.; Wolf, M. E. *J. Am. Chem. Soc.* **1973**, *95*, 2865–2868.
(16) Maudsley, A. A.; Wokaun, A.; Ernst, R. R. *Chem. Phys. Lett.* **1978**, *55*, 9–14.
(17) Pegg, D. T.; Doddrell, D. M.; Bendall, M. R. *J. Chem. Phys.* **1982**, *77*, 2745–2752.
(18) Morris, G. A.; Freeman, R. *J. Am. Chem. Soc.* **1979**, *101*, 760–762.
(19) Burum, D. P.; Ernst, R. R. *J. Magn. Reson.* **1980**, *39*, 163–168.
(20) Aue, W. P.; Karhan, J.; Ernst, R. R. *J. Chem. Phys.* **1976**, *64*, 4226–4227.

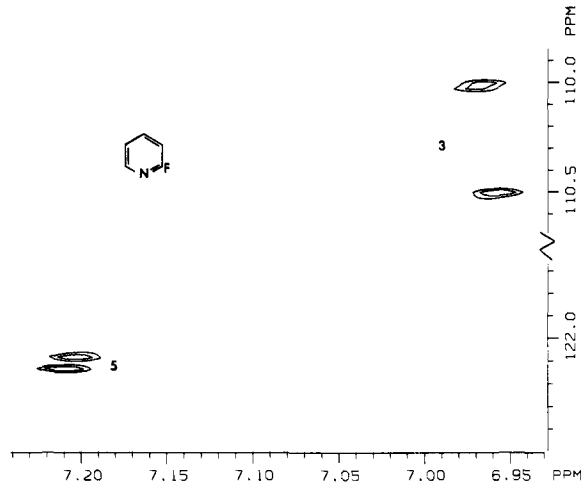

Figure 2. Part of the ^1H–^{13}C chemical shift correlation map of 2-fluoropyridine. Since homonuclear J couplings have been eliminated by the selective flip of distant protons, positions of peaks are determined by chemical shifts and heteronuclear J couplings with the additional (^{19}F) spin. The map clearly shows that J_{H_5F} and J_{C_5F} have the same sign, while for the CH spin pair of position 3 one of the couplings with fluorine must be negative.

MHz) give rise to reliable ^1H chemical shift determinations. On the other hand, it must be stressed that any 2-D acquisition of low-sensitivity ^{13}C signals requires longer spectrometer time, and signal-to-noise ratio becomes especially critical when nonequivalent protons are attached to the same carbon, thus splitting resonances along the F_1 dimension.

Heteronuclear chemical shift correlation maps obtained by pulse sequences A and C are not limited to measurements of ^1H chemical shifts and geminal couplings. If an additional nucleus X with spin $^1/_2$ (X = ^{19}F, ^{31}P,...) is present, its couplings with ^1H and ^{13}C spins show up in a unique way.[21] Let us suppose that the ^{13}C spin is coupled to the X nucleus in the "up" state and that the resonance peak is shifted to $\delta_C + {}^1/_2J_{CX}$ where δ_C and J_{CX} denote chemical shift and heteronuclear J coupling, respectively. The attached proton must be coupled to the X spin in the same state; therefore, the peak is found at $\delta_H + {}^1/_2J_{HX}$ along the F_1 dimension. Similar arguments apply to the "down" state of the X nucleus, and resonances are shown as pairs of peaks at ($\delta_H + {}^1/_2J_{HX}$, $\delta_C + {}^1/_2J_{CX}$) and ($\delta_H - {}^1/_2J_{HX}$, $\delta_C - {}^1/_2J_{CX}$) in the correlation map (Figure 2). Splittings along the F_1 dimension reveal coupling between ^1H and additional spin even without resolving homonuclear coupling patterns which can be quite complicated in complex molecules. Furthermore, relative signs of coupling constants are determined: if the peaks are shifted in the same direction along both dimensions, J_{HX} and J_{CX} have the same sign, while the opposite directions mean that one of the couplings is negative while the other positive. Several simple compounds bearing one or more fluorine nuclei, 2-fluoropyridine, 2,5-difluoroaniline, and difluorobenzenes, have been used in this study to test and demonstrate the utility of pulse sequences A and C in deciphering the magnitude and relative sign of ^1H–X couplings from the correlation map.

Experimental Section

About 50% (v/v) solutions of 2-fluoropyridine, 2,5-difluoroaniline, and difluorobenzenes in $CDCl_3$ in 5-mm tubes were used. To generate a 256 × 2K data set for these samples, 1.5–2 h of acquisition time was required. A total of 10 mL of a 0.25 M solution of **1** in Me_2SO-d_6 was used in a 20-mm probe. Approximately 11 h were required to accumulate a 256 × 2K data set, which was generated by incrementing the evolution time t_1 in steps of 600 μs. The relatively long data acquisition times were mainly due to the large number of data sets (256) acquired to make full advantage of the inherently higher resolution offered by this method over the conventional heteronuclear chemical shift correlation method. 1-D spectra of all samples were taken of the same solutions in a 5-mm probe.

(21) Rutar, V. *Chem. Phys. Lett.* **1984**, *106*, 258–261.

Table II. ^1H Chemical Shifts and Heteronuclear Couplings with ^{19}F in 2-Fluoropyridine[a]

position	δ (^1H), ppm	J_{HF}, Hz
3	6.956[b]	−2.4[c]
4	7.816	8.5
5	7.201	1.9
6	8.235	−1.0

[a] As measured by ^1H–^{13}C chemical shift correlation spectroscopy. [b] Accuracy ±0.002 ppm. [c] Accuracy ±0.5 Hz.

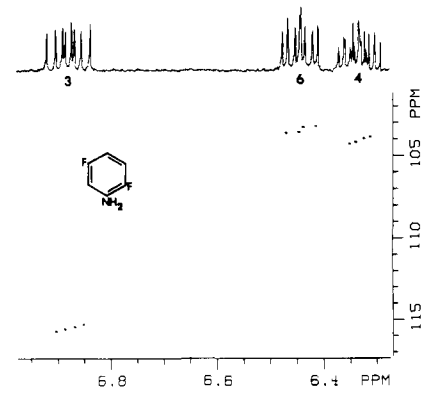

Figure 3. ^1H–^{13}C chemical shift correlation map of 2,5-difluoroaniline where ^{13}CH spin pairs are coupled to two nonequivalent ^{19}F spins. Suppression of homonuclear J couplings simplifies determinations of heteronuclear couplings with ^{19}F. The upper trace shows 1-D ^1H spectrum for comparison.

All spectra were taken on a Nicolet NT-300 spectrometer (^1H frequency 300.05 MHz; ^{13}C frequency 75.45 MHz). The $\pi/2$ pulse widths used in pulse sequences A and C are 60 μs for ^1H and 45 μs for ^{13}C for the 20-mm probe and 30 and 12 μs, respectively, for the 5-mm probe. Large-volume NMR probes with saddle coils are notorious for imperfect radio-frequency pulses, and we noticed that pulse sequence A gave rise to slighly worse signal-to-noise ratio and it also increased the intensity of some spurious peaks which somewhat offset the convenience of the phase sensitive display. The experiment was repeated by using pulse sequences C and A with and without the refocusing pulses. Since ^{13}C signals of C_8 (split by ^{19}F) and C_2 partially overlap along the F_2 dimension, the spectral editing capability of sequence A was also utilized by changing the pulse θ from $\theta_1 = \pi/4$ to $\theta_2 = 3\pi/4$.

After Fourier transformation with respect to the acquisition time t_2 to separate ^{13}C signals along the F_2 dimension, only 32 data points around each ^{13}C peak, instead of the whole data set, were transposed to avoid limitations imposed by the size of the computer memory. Further processing included digital apodization, zero-filling up to 8K data points, and Fourier transformation with respect to the evolution time t_1 to obtain cross sections for ^1H signals along the F_1 dimension. The processing time for a 256 × 2K data set for **1** is about 1 h on a Nicolet 1280 computer.

The ^1H chemical shifts were calibrated with respect to the C_{18} methyl proton signal at 0.750 ppm and are accurate to within 0.005 ppm.

Results

2-Fluoropyridine, 2,5-Difluoroaniline, and Difluorobenzenes. The correlation map obtained for 2-fluoropyridine shows how the magnitude and the relative sign of ^1H–^{19}F couplings can be determined in addition to the ^1H chemical shifts. Figure 2 shows contour plots for 2-fluoropyridine where couplings of C_5 and H_5 with ^{19}F are of the same sign, but $^3J_{H_3F}$ and $^2J_{C_3F}$ are of opposite signs. Experimental results (Table II) agree with previous studies[22,23] using double resonance techniques.

In 2,5-difluoroaniline two nonequivalent fluorine nuclei are present and the ^1H–^{13}C chemical shift correlation map (Figure 3) reveals four peaks for each CH group. Projection onto the F_2 dimension is equivalent to the 1-D $^{13}C\{^1H\}$ spectrum, while cross sections along the F_1 dimension give rise to "proton-decoupled" ^1H resonances which show only couplings with ^{19}F spins. Ex-

(22) Thomas, W. A.; Griffin, G. E. *Org. Magn.* Reson. **1970**, *2*, 503–510.
(23) Brey, W. S.; Jaques, L. W.; Jakobsen, H. J. *Org. Magn. Reson.* **1979**, *12*, 243–246.

Table III. ^1H Chemical Shifts and Heteronuclear Couplings with ^{19}F in 2,5-Difluoroaniline[a]

	δ (^1H),[b] ppm	J_{HF},[c,d] Hz
H_3	6.877	$^3J_{H_3F_2} = 10.6$ $^4J_{H_3F_5} = 5.1$
H_4	6.332	$^3J_{H_4F_5} = 8.2$ $^4J_{H_4F_2} = 3.4$
H_6	6.442	$^3J_{H_6F_5} = 9.7$ $^4J_{H_6F_2} = 7.2$

[a] Measured by ^1H–^{13}C chemical shift correlation spectroscopy. [b] Accuracy ±0.002 ppm. [c] Accuracy ±0.3 Hz. All HF couplings are of the same sign as the corresponding CF couplings. [d] In each case, the larger value has been assigned to the three-bond coupling.

perimental results are summarized in Table III. The contour plot (Figure 3) facilitates assignment of peaks, and it also shows that the couplings $J_{H_nF_m}$ have the same signs as the associated couplings $J_{C_nF_m}$ (n = 3, 4, 6,; m = 2, 5). No information on the ^1H–^{19}F couplings of this compound was available in the literature. However, both the sign and magnitude of the present results are in excellent agreement, with corresponding couplings obtained for other difluoroanilines by double resonance techniques.[24]

Thus, heteronuclear chemical shift correlation maps can be used for separate measurements of couplings between ^1H and ^{19}F (or other) spins. The results are easily assigned, and determination of relative signs of coupling constants does not require tedious spin-tickling or double resonance experiments. This advantage is somewhat offset by the fact that 2-D data sets generally do not provide the same line widths as 1-D spectra. Even in worst cases, however, the values of $\delta(^1H)$ and J_{HF} can be utilized as starting parameters which significantly simplify subsequent simulation of the 1-D ^1H spectrum.

A peculiar case is faced when two chemically equivalent ^{19}F spins are present in molecules such as 1,3-difluorobenzene. If the additional nuclei are symmetrical with respect to the ^{13}CH pairs, the suppression of homonuclear couplings reveals a triplet along the F_1 dimension, and $^3J_{H_2F} = 9.3$ Hz and $^4J_{H_5F} = 6.6$ Hz are determined immediately from the splitting. On the other hand, the presence of the ^{13}C nucleus at position 4 (or 6) induces isotope shifts of fluorine resonances which have to be taken into account if one wants to derive J_{HF} couplings from the proton-decoupled indirect spectrum of H_4.

9α-Fluorocortisol. Several signals in the 4–5 ppm region in the proton spectrum of **1** can be assigned from the 1-D spectrum. Proton H_4 gives rise to a downfield resonance at 5.666 ppm with a small coupling of 2.1 Hz most likely with $H_{6\beta}$. Protons at position 21 are nonequivalent, and they contribute to peaks at 4.09 and 4.52 ppm which are split by geminal coupling $^2J_{HH} = 19.1$ Hz and coupling of 5.7 Hz with the neighboring OH group. The other two signals of the OH groups are sharp. Under one half of the doublet of H_{21} at ~4.1 ppm lies another peak which was later assigned to H_{11} by the correlation spectroscopy (Figure 4). Methyl protons 18 and 19 give rise to single peaks at 0.750 and 1.480 ppm, while all other signals could not be easily identified.

^{13}C chemical shifts and J couplings between ^{13}C and ^{19}F (F_2 dimension) have been measured and assigned previously;[25] therefore, cross sections along the F_1 dimension unambigously reveal ^1H chemical shifts and geminal couplings. It is obvious from the inspection of cross sections along the F_1 dimension that nonequivalent methylene protons give rise to the worst signal-to-noise ratio, because the resonances are split into four peaks due to chemical shift difference and geminal coupling. The intensity is further decreased by missetting of the delay τ, strong coupling, and partial flip of distant protons.[13] It is, therefore, not surprising that the worst results were obtained for protons attached to C_7 and C_{15} which are coupled to many neighboring ^1H spins.

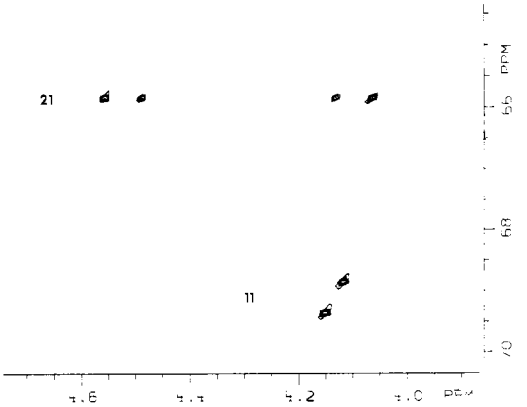

Figure 4. Portion of the ^{13}C–^1H chemical shift correlation map of **1**. For C_{21}, the chemical shifts for the two nonequivalent protons and the $^2J_{HH}$ between them are observed along the F_1 dimension. For C_{11}, the signal is split by J_{HF} and J_{CF}. The direction of the doublet shows that $^3J_{H_{11}F}$ and $^2J_{C_{11}F}$ are of the same sign.

Table IV summarizes experimental results which were derived from 2-D heteronuclear chemical shift correlation spectroscopy of **1**. Reported values represent averages from independent measurements via different versions (pulse sequences A or C) which gave rise to reproducible patterns even for those cross sections where the signal-to-noise ratio or resolution was marginal.

Discussion

Chemical Shift. The effect of fluorine substitution on the ^1H chemical shift can be discerned by comparing the ^1H chemical shifts between **1**. 11β-hydroxyprogesterone (**2**),[2] 6α-methyl-17α-acetoxyprogesterone (**3**),[3] and progesterone (**4**),[14] particularly in rings B and C with **2**, and in ring D with **3**. The proton chemical shifts of **2**, **3**, and **4** are included in Table IV for comparison. The chemical shift of protons at positions relatively unaffected by substitution showed good agreement among these molecules. Thus, $\delta(^1H)$ of protons 6α, 6β, 7α, 2α, and 2β are found to be within 0.1 ppm of the corresponding ones in **2** and **4**. Likewise, $\delta(^1H)$ of protons 15α and 15β agree with those in **3**. The differences in the δ (^1H) of 16α and 16β between **1** and **3** basically reflect the different effects of the OH and the OAc groups in position 17α and the effect of the additional substitution of an OH group in position 21. The major effects of the fluorine substitution are felt by protons at positions 7α and 14 where a downfield shift in **1** of about 1.2 and 1.0 ppm, respectively, was observed. This downfield shift arising from the 1,3-diaxial interaction is consistent with the expected direction.[1] Similarly, a smaller downfield shift should be observed for vicinal axial protons and a small upfield shift for vicinal equatorial protons.[1] Thus $\delta(^1H)$ for H_8 was observed to be downfield by 0.3 ppm and for H_{11} upfield by 0.27 ppm. The chemical shifts of 12α and 12β are affected slightly bu substitutions both in positions 9 and 17. The combined effects resulted in upfield shifts of ca. 0.2 and 0.1 ppm, respectively, for the α and β protons. The $\delta(^1H)$ of protons 1 and 2 in the A ring will be discussed in a later section on the conformation of the A ring.

^1H–^{19}F and Geminal ^1H–^1H Coupling Constants. In addition to the proton chemical shifts ^1H–^{19}F as well as the geminal ^1H–^1H coupling can be obtained along the F_1 dimension. Thus for H_8 and H_{11} in **1**, which are three bonds away from F_9, large ^1H–^{19}F coupling is expected.[26] Indeed, the signals of these protons in the F_1 dimension were clearly observed to be split, and $^3J(^1H_8$–$^{19}F)$ and $^3J(^1H_{11}$–$^{19}F)$ were found to be 32.8 and 10.4 Hz, respectively. These values are consistent with what is expected for the cases of F_{ax}–H_{ax} and F_{ax}–H_{eq} in cyclohexyl rings.[26] The latter is also in good agreement with the value of 9 Hz observed for 9α-fluoro-11β-hydroxyprogesterone.[1] Furthermore, it can be established from the ^{13}C–^1H chemical shift correlation map that

(24) Abrahams, R. J.; McDonald, D. B.; Pepper, E. S. *J. Chem. Soc. B* **1967**, 835–841. Abrahams, R. J.; Copper, M. A. *Ibid.* **1968**, 1094–1098.
(25) Giannini, D. D.; Kollman, P. A.; Bhacca, N. S.; Wolff, M. E. *J. Am. Chem. Soc.* **1974**, *96*, 5462–5466.
(26) Emsley, J. W.; Philip, L.; Wray, V. *Prog. Nucl. Magn. Reson. Spectrosc.* **1976**, *10*, 85–576.

Table IV. ^{13}C and ^{1}H Chemical Shifts (in ppm), $^{2}J_{HH}$ and J_{HF} (in Hz), of **1** and ^{1}H Chemical Shifts of **2**, **3**, and **4**

carbon no.[d]	1					2[a]	3[b]	4[c]
	$\delta(^{13}C)$	$^{2}J_{HH}$		J_{HF}	$\delta(^{1}H)$[e]	$\delta(^{1}H)$	$\delta(^{1}H)$	$\delta(^{1}H)$[e]
1	25.97	14.4 ± 1	α		1.403	1.84	1.70	1.716
			β		1.722	2.18	2.03	2.047
2	33.44	15.4 ± 1	α		2.218	2.35	2.35	2.337
			β		2.416	2.47	2.43	2.441
4	123.84				5.666	5.67	5.80	5.730
6	30.17	16.0 ± 1	α		2.236	2.23		2.280
			β		2.557	2.48	2.42	2.412
7	27.74	15.1 ± 2	α		2.249	1.06	0.88	1.065
			β		1.973	2.0	1.85	1.870
8	33.66		β	32.8 ± 0.5	2.291	1.98	1.69*	1.570
9	100.00		α			1.00	1.01	0.989
11	69.10		α	10.4 ± 0.5	4.133	4.40	1.67	1.645
			β				1.42	1.461
12	35.44	15.5 ± 1	α		1.450	1.65	1.95	1.456
			β	~2	2.146	2.21	1.56	2.079
14	44.99		α		2.107	1.11	1.65*	1.181
15	23.16	14 ± 3	α		1.621	1.75	1.65	1.724
			β		1.268	1.33	1.29	1.267
16	32.95	16.2 ± 1	α		1.439	1.69	1.65	1.676
			β		2.584	2.17	2.93	2.189
18	16.46				0.750	0.90	0.67	0.669
19	21.32				1.480	1.44	1.18	1.196
21	65.88	19.5 ± 1[f]			4.095	2.11	2.03	2.127
					4.521			

[a] From ref 3. [b] From ref 4; the assignments marked with * have been disputed in ref 14. [c] From ref 14. [d] Only protonated carbons have been included. [e] Estimated uncertainty ±0.005 ppm. [f] 19.1 ± 0.1 Hz from 1-D spectrum.

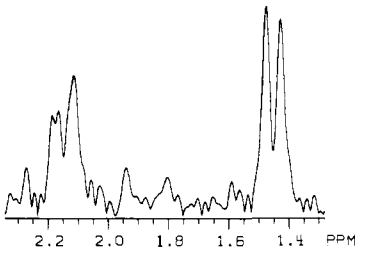

Figure 5. Cross section along the F_1 dimension showing that two chemically nonequivalent protons $H_{12\alpha}$ and $H_{12\beta}$ are attached to the same carbon C_{12}. Selective reversal of distant protons does not eliminate the geminal coupling. Additional small splitting of the low-field proton doublet ($H_{12\beta}$) is due to heteronuclear coupling with fluorine, $^{4}J_{H_{12\beta}F} \sim 2$ Hz.

both ^{1}H–^{19}F couplings are of the same sign as those of the corresponding ^{13}C–^{19}F couplings (Figure 4).

At least one four-bond ^{1}H–^{19}F coupling has been observed. The cross section along the F_1 dimension for C_{12} is shown in Figure 5. It is clear that the lower field doublet corresponding to proton 12β is broader and small splitting is observed on the outside peak. Unfortunately, the relatively poor resolution prevented accurate measurement of this coupling ($^{4}J_{H_{12\beta}F} = 2 \pm 1$ Hz). The sign of this coupling is unknown, because the attached carbon C_{12} has no resolvable coupling with fluorine. Other four- or five-bond $J(^{1}H$–$^{19}F)$ may be present in several proton signals ($H_{7\beta}$, $H_{2\beta}$). These proton peaks are found to be broader than the corresponding ones in **4**, for example. However, these couplings are about 1 Hz or less. Very little is known about ^{1}H–^{19}F couplings in fluorinated steroids,[1] with probably the exception in ^{19}F–methyl proton couplings.[27] Hall and co-workers[28] have shown that fluorine at axial positions in fluorinated sugars does not have as large long range (four- or five-band) ^{1}H–^{19}F coupling as fluorine at equatorial positions. If the same situation applies to six-membered rings in steroids, the long-range ^{1}H–^{19}F couplings involving the axial F_9 in **1** would be expected to be small and most likely would not be resolved.

Conformation of the A Ring. The ^{1}H chemical shifts of protons 1α and 1β are both about 0.3–0.4 ppm upfield from the corresponding ones in **2**, **3**, and **4**. Weeks et al.[15] from the X-ray studies reported a bending of the A ring in **1** further below the average plane of the molecule than in cortisol and related steroids. This bending serves to relieve the close nonbonded contact of F_9–$H_{1\alpha}$ and can be accomplished by rotating along the C_1–C_{10} bond. Thus, the C_2–C_1–C_{10}–C_9 dihedral angle was found to be 155° in **1** as compared to 165° in cortisol and several other analogues.[15] This rotation along the C_1–C_{10} bond changes the orientation of the methyl 19 with respect to the protons 1α and 1β to one closer to an equatorial methyl group, which is known to cause an upfield shift of 0.3–0.5 ppm for both the axial and equatorial protons on the adjacent carbon[29] (1α and 1β in this case). However, according to the Dreiding model we have constructed, an inverted A ring[30] would probably cause a similar upfield shift in $\delta(^{1}H)$ of protons 1α and 1β. Besides the unusual upfield shift of $\delta(^{1}H)$ of 1α and 1β, there is supporting evidence for an "abnormal" A ring conformation: H_{19}(methyl)–$H_{1\alpha}$ coupling, which is frequently found in steroids with normal A ring conformation (W rule),[3] was not observed in the present study of **1**. In addition, the $\delta(^{1}H)$ and $^{2}J_{HH}$ of protons 2α and 2β also differ from those of **2**–**4**. In **2**–**4**, proton 2α and 2β are close to being symmetrically disposed with respect to the plane defined by the $C_5{=}C_4{-}C_3{=}O$ fragment in the normal A ring structure. Therefore the $\delta(^{1}H)$ of protons 2α and 2β were found to be ~0.1 ppm with each other. Similarly in normal A rings, $^{2}J_{HH}$ between protons 2α and 2β being next to the carbonyl group ranges from 17.7 and 17.3 Hz for **4** and **2** to 16.2 Hz in **3** (which has an inverted A ring in the crystalline form).[3] The relatively large magnitude of $^{2}J_{HH}$ arises from a large contribution from the neighboring carbonyl group because the orientation of the methylene protons 2 with respect to the π bond of the carbonyl group is close to the optimal orientation (~30°).[31,32] However, when the A ring is in the inverted conformation or in the form proposed from the X-ray result,[15] the

(27) Cross, A. D.; Landis, P. W. *J. Am. Chem. Soc.* **1962**, *84*, 3784–3785; **1965**, *86*, 4005–4010.
(28) Foster, A. B.; Hems, R.; Hall, L. D.; Manville, J. F. *Chem. Commun.* **1968**, 158–159. Foster, A. B.; Hems, R.; Hall, L. D. *Can. J. Chem.* **1970**, *48*, 3937–3945.
(29) Booth, H. *Tetrahedron*, **1966**, *22*, 615–620.
(30) Duax, W. L.; Norton, D. A. "Atlas of Steroid Structure"; Plenum: New York, 1975; Vol. 1.
(31) Barfield, M.; Grant, D. M. *J. Am. Chem. Soc.* **1963**, *85*, 1899–1904.
(32) Williams, D. H.; Bhacca, N. S. *Chem. Ind.* **1965**, 506–507.

positions of 2α and 2β become farther away from being symmetrical with respect to the C=C—C=O plane, and the orientation of the methylene group at C_2 makes a different angle with the π orbital of the C=O group. Thus the difference in the $\delta(^1H)$ of the protons 2α and 2β are expected to increase and the magnitude of $^2J_{HH}$ of protons 2 will decrease. Indeed, the difference of $\delta(^1H)$ of 2α and 2β was found to be 0.2 ppm and $^2J_{HH}$ decreases markedly to 15.4 Hz.[33] Although the changes associated with protons at position 2 are small, together with the upfield shift of $\delta(^1H)$ of protons 1, they suggest that *in solution*, an inverted conformation or a conformation similar to that found in crystal for the A ring is the predominant one for **1**. One has to be cautious in making conclusions based on proton chemical shifts which are dependent on solvent and anisotropy. However, the present results are consistent with the notion that steroid conformations are usually unchanged between crystal and solution states.

(33) This decrease in $^2J_{HH}$ of H_2 and its conformational implications are firmly substantiated by a separate study in which $^2J_{HH}$ for a series of substituted progesterones, including **1**, were selectively measured via an indirect J spectroscopy with much higher accuracy (Wong, T. C.; Clark, G. R. *J. Chem. Soc., Chem. Commun.*, in press). The change of $^2J_{HH}$ of H_2 was found to agree perfectly with theoretical predictions (ref 31) based on structures determined from X-ray diffraction.

Conclusion

This study of a relatively complex molecule **1** demonstrates again that indirect homonuclear decoupling gives rise to useful ^1H–^{13}C chemical shift correlation maps. Measurements of ^1H chemical shifts, geminal couplings $^2J_{HH}$, and heteronuclear couplings with the additional spin support our opinion that the described 2-D NMR technique provides more pertinent information than the traditional versions of heteronuclear chemical shift correlation.

Acknowledgment. The NT-300 spectrometer was purchased partially through a grant from the National Science Foundation (PCM-8115599). This work is partially supported by the National Institutes of Health Institutional Biomedical Research Support Grant RR07053. Helpful discussion with Dr. Elmer Schlemper is gratefully acknowledged.

Registry No. 1, 127-31-1; **2**, 600-57-7; **3**, 71-58-9; **4**, 57-83-0; 2-fluoropyridine, 372-48-5; 2,5-difluoroaniline, 367-30-6; 1,2-difluorobenzene, 367-11-3; 1,3-difluorobenzene, 372-18-9; 1,4-difluorobenzene, 540-36-3.

Carbon Monoxide Activation by Organoactinides. A Comparative Synthetic, Thermodynamic, Kinetic, and Mechanistic Investigation of Migratory CO Insertion into Actinide–Carbon and Actinide–Hydrogen Bonds To Yield η^2-Acyls and η^2-Formyls

Kenneth G. Moloy and Tobin J. Marks*

Contribution from the Department of Chemistry, Northwestern University, Evanston, Illinois 60201. *Received April 5, 1984*

Abstract: This paper reports the synthesis, characterization, and carbon monoxide chemistry of a series of sterically hindered thorium alkyls and hydrides of the type $Cp'_2Th(R)(X)$ ($Cp' = \eta^5$-C_5Me_5) where R = H, D, Me, *n*-Bu, and CH_2-*t*-Bu and X = OCH-*t*-Bu_2, OC_6H_3-2,6-*t*-Bu_2, and O-*t*-Bu. In addition, improved syntheses of the known complexes $[Cp'_2Th(\mu\text{-}H)(H)]_2$, $Cp'_2Th(O\text{-}t\text{-}Bu)(Cl)$ and $Cp'_2Th(CH_2\text{-}t\text{-}Bu)(Cl)$ are presented. The alkyl complexes undergo facile, irreversible carbonylation to yield η^2-acyls that were characterized by a variety of methods. Infrared and ^{13}C NMR spectra of these complexes demonstrate that strong metal–(acyl)oxygen bonding takes place, fostering a pronounced carbene-like character. Thus, these complexes are characterized by low C–O infrared stretching frequencies (ν_{CO} = 1450–1480 cm^{-1}) and low-field ^{13}C NMR chemical shifts ($\delta_{^{13}C}$ 355–370). The hydrides undergo a rapid, reversible, migratory CO insertion to yield formyls that have been characterized spectroscopically at low temperature. Infrared and ^{13}C NMR spectra of these species are quite similar to the corresponding acyls, suggesting an analogous η^2 structure. Variable-temperature equilibrium data show that the insertion of CO into thorium–hydrogen bonds is exothermic by ca. 5 kcal/mol, and this value is compared to that for the analogous alkyls. The equilibrium was also found to exhibit a distinct equilibrium isotope effect upon deuterium substitution, $K_H/K_D = 0.31$ at −78 °C. The carbonylation of the complex $Cp'_2Th(n\text{-}Bu)(OCH\text{-}t\text{-}Bu_2)$ was found to obey a second-order rate law where rate = kP_{CO}[complex]. Likewise, the insertion of CO into the Th–H bond of $Cp'_2Th(H)(OCH\text{-}t\text{-}Bu_2)$ was found by NMR methods to be first order in metal hydride. Labeling and crossover experiments offer further support for an intramolecular pathway for CO insertion, resulting in the formation of monomeric formyls. The insertion exhibits a primary kinetic isotope effect; at −54 °C, $(k_H/k_D)_{forward} = 2.8$ (4) (insertion) and $(k_H/k_D)_{reverse} = 4.1$ (5) (extrusion). Thus, the insertion is inferred to involve rate-determining migration of the hydride ligand. Approximate rate data for the series of alkyls synthesized show that the rate of hydride migration greatly exceeds that of alkyl migration. For the complexes reported herein, $k(H) \approx 5 \times 10^3 k(CH_2\text{-}t\text{-}Bu) \approx 7 \times 10^4 k(n\text{-}Bu) \approx 10^8 k(Me)$. The latter three rates partially mirror Th–C bond disruption enthalpy trends. The rate of migratory insertion is impeded when the steric bulk of the alkoxide coligand is increased and accelerated when it is replaced by chloride.

One of the most well-studied and important reactions in all of inorganic/organometallic chemistry involves the migratory insertion of carbon monoxide into a metal–alkyl bond to yield an acyl complex (eq 1).[1] Transformations such as this have enormous

0002-7863/84/1506-7051$01.50/0 © 1984 American Chemical Society